FAULT DETECTION SCHEME OF 5 BUS BY ANN AND ANFIS

Mr. Payal Ingole[1], Assst .Prof. A. V. Mohod[2]

[1]Student, Prof Ram Meghe College of Engineering and Management, Badnera
[2]Asst.Prof. Prof Ram Meghe College of Engineering and Management, Badnera

---

***ABSTRACT**: In micro grid control and operation, failure detection is essential because it makes the system quick to isolate and recover from the fault. Due to the use of inverter-interfaced distributed generation in microgrids, standard fault detection systems are no longer appropriate because they rely on large fault currents. We propose an intelligent microgrid fault detection technique based on wavelet transform neural networks and ANFIS in this paper. The scheme uses a discrete wavelet to pre-process branch current measurements sampled via VI Bus measurement for extracts statistical features. Then all available data are entered into deep neural networks to generate false data. The proposed scheme can offer significantly improved fault-type classification precision compared to previous work. In addition, the system can detect fault locations that are not available in previous work. A comprehensive evaluation study on the CERTS microgrid and the IEEE 5 bus system is undertaken to evaluate the performance of the proposed failure detection scheme. The results of the simulation demonstrate the effectiveness of the proposed scheme in terms of detection accuracy, computer speed and measurement uncertainty robustness.*

***Index Terms*—Fault detection, fault location, microgrid protection, wavelet transform, neural network.**

INTRODUCTION:

Due to progress in Distributed Generation (DG) development [1], microgrids are gathering attention from industry and research community. Thanks to improved power efficiency, reliability and quality, these will bring advantages to modern power system control. Microgrids can be operated on either grid-connected or in the Icelandic mode if the external grid suffers from disruptions like deviations of frequency and voltage fluctuations. Critical loads in microgrids can be supplied without the external grid in island mode by load-side DGs. In the meantime, microgrid protection is one of the main and critical tasks[1]–[3]. With the progressive use in modern power systems of renewable energy sources, micro-grids are commonly integrated with interface DGs, such as PVDG and battery energy storage systems. inter-face DGs are also commonly integrated (BESS). Large fault currents depend on traditional protective relays for distribution system fault detection. However, only negligible fault currents can contribute to IIDG's that protect schemes are not enabled[4]. These relays can therefore not protect microgrids. [5] provides a detailed analysis of the dynamics of current and voltage in such microgrids. Microgrid failure detection usually has three goals. If the system has a fault, the type of fault (e.g. single-phase-to-ground, three-phase-short, etc.) should be determined, and the fault phase should be determined. The first two enable isolation operations for fault subsequently, and the latter can be restored to service. According to [5], the operation of sound stages in unbalanced short circuit errors in order to support the integration of one-stage protection devices should continue with modern microgrids. Selective phase tripping can be achieved given accurate fault type and fault phase information[6]. As a result, the reliability of sys-tems is improving significantly [7], and this protection system is being gradually adopted by utilities [8]. In addition, accurate detection of the failure location can considerably reduce service restoration efforts[9], which is increasingly important if underground operations are to be restored.

Data and digital signal processing methods for microgrid fault type or phase detection are used in recent years by a growing number of researchers. For example, random tree and random forest are often used to detect faults in both the networked and insulated microgrid systems (see example for [4], [10]–[12]). For the detection of defects in the literature[3] [12] also have been used other machine learning techniques e.g. vector support and algorithms of neighbouring k-nearest. Due to these data-driven approaches' high calculation speed, satisfactory fault classification can be developed nearly in real time. Furthermore, in order to better exploit the time-frequence properties for analyzes [3],[4],[12], digital signals processing approaches such as discrete Fourier transform and discrete Wavelet (DWT) are used for "pre- processing" input signals. For investigations of microgrid fault detection plans in the literature, interested readers may refer to [1] and [4]. In the development of microgrid fault detection programmes, however, there remains a research gap. Some existing research cannot provide information about the fault type and cannot therefore be properly adopted in the trip paradigm of the single phase (see [12], [13] for examples). In addition, current work on detecting fault locations focuses on microgrids with low-voltage CDs, e.g. [14], [15]. The location fault can normally be identified by travelling or injection-driven algorithms in AC distribution network [9], [16]. Traveling wave algorithms, however, are affected by reflected wave detection problems and problems of discrimination[14],[17], some of which require synchronised communication link data[18] No fault locating performance on islanded microgrids and loop/ring topology networks was demonstrated by either. Meanwhile, phase-to-ground faults are the sole applicable injection-based algorithms in the radial

networks [14]. This article presents a smart failure detection system based on DWT and the recent development of deep neural networks (DNN), a class of machine learning techniques driven by data to overcome a fault detection gap for IIDG-enabled microgrids. Whereas DWT is likely to cause noise and power disturbances, DNN is introduced with the exceptional ability of DNN to handle noise data [19][20] to improve its robustness The scheme of fault detection scheme is presented in Fig. 1. Fig. 1. The system uses current magnitudes of three phases in a cycle, which are sampled as input data via protective relays. DWT processes the measurements to remove the time-frequency domain functionalities. In addition, the measurements will then be included in three DNNs for classification of fault type, identification of fault phase and detection of fault locations. Finally, information about the fault is developed, which can be used in subsequent protection and remedial control measures. This report summarizes the contributions of:

We propose an IEEE 5 BUS system failure detection mechanism to provide accurate and expedited information about the defect type, phase and location;

- ANN and ANFIS are combined with DWT in order to resolve the data-driven microgrid failure detection problem;
- We conduct extensive case studies to analyse the performance of the mechanism proposed and compare the results with the latest technology.
- The proposed detection results can be accurate and quick (type, phase, and location) without communications compared with existing defect detection mechanisms. It can be adapted to various operating modes, network topologies and radiale and loop topology, for example grid-connected, isolated mode. Power dynamics can also be handled with both conventional and IIDG synchronous generators. Discrete Wavelet Transform (DWT).

The FT does not provide direct data for a signal oscillating and is suitable for investigating the problems of the constant state. STFT divides the full time interval into several small/equal intervals, which will be analysed separately by FT. However, it is ineffective to detect very short and high frequency signals via STFT. Due to its diverse window function for the time domain, the WT has been used widely to analyse passing signals. The WT prevents the FT and STFT inconveniences. The DWT version of WT is extended and uses discreet time signals. The DWT breaks the signal down by ·(t) and¨. (t). The DWT application requires the calculation of discrete c(k) and dj filter banks (k). A low-pass filter H and a high-pass filter g[25] decompose the signal. A factor of 2 A is then sampled for the filtered signal.

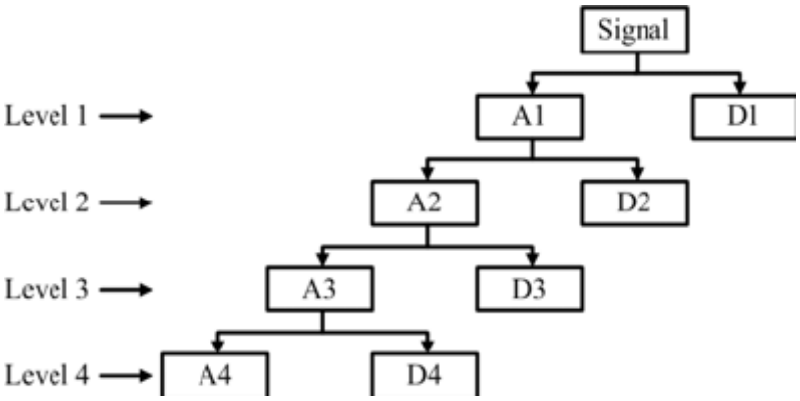

Fig:1 4 level Three-scale signal decomposition

Methodology:

Artificial Neural Network

The structure of an ANN must be simple and efficient for solving the problem to implement an ANN in a chip. The ANN is carried out because it has the capacity to learn. The works presented in [2], [8], [10], [11], [16], [17], [19] can therefore be avoided in their demerits. The ANN used in the paper is a three-faceted network with seven inputs [28]: difference between the two- and three-phase-voltage (VA−B, VB−C, VA−C) added wavelet entropies, the difference between the phase current (IA-00B, IB−C, IA−C), and the neutral-current entropy wavelet; (Ig). The ANN has a cached layer and a layer of output. Fig. 4 displays the structure of the neural network. The neural network is able to identify 11 types (single-phase to-ground, unbalanced two-phase, and balanced faults) of faults occurring at the grid side, Zone A, or Zone B. As shown in Fig. 4, there are one neuron at the output layer: to localize, classify and identify the fault in this paper 3 ANN is connect

ANN1 HAS 10 INPUT AND 10 OUTPUTS

ANN2 HAS 10 INPUT AND 5 OUTPUTS,

ANN3 HAS 5 INPUT AND 2 OUTPUTS

Thus, the studied faulty locations are only three and are given in Fig. 2. The architecture of the ANN (e.g., the number of hidden layers) is decided generally by heuristics [28]. More hidden layers tend to attain a good fitting but are most likely to be overfitting. This implies that the ANN fits too well to the training set but does not perform well on the testing set.

Adaptive network fuzzy inference systems

To illustrate the use of neural networks for fuzzy inference, we present some successful adaptive neural network fuzzy inference systems, along with training algorithms known as ANFIS. These structures, also known as adaptive neuro-fuzzy inference systems or adaptive network fuzzy inference systems, were proposed by Jang [35]. It should be noted that similar structures were also proposed independently by Lin and Lee [40] and Wang and Mendel [77]. These structures are useful for control and for many other applications.

To fix the ideas, consider the problem of graphically representing the way fuzzy control is achieved in the Sugeno-Takagi model. For a simple example, consider a fuzzy rule base consisting of only two rules:.

R1: If x1 is A1 and x2 is B1 then y = f1 (x)

R2: If x1 is A2 and x2 is B2 then y = f2 (x)

Where, Ai and Bi are fuzzy sets and

f1 (x) = z11x1 + z12x2 + z13

f2 (x) = z21x1 + z22x2 + z23

Recall that when numerical input x = (x1, x2) is presented, the inference mechanism will produce the numerical output

$$y^* = \frac{A_1(x_1)\,B_1(x_2)\,f_1(\mathrm{x}) + A_2(x_1)\,B_2(x_2)\,f_2(\mathrm{x})}{A_1(x_1)\,B_1(x_2) + A_2(x_1)\,B_2(x_2)}$$

A fuzzy-neural network for implementing the above is shown in figure 3.2. The observed input x = (x1, x2) is presented to Layer 1 by Input Layer 0. The output of Layer 1 is

(O11, O12, O13, O14) = (A1 (x1), A2 (x1), B1 (x2), B2 (x2))

Where, the membership functions Ai, Bi, i = 1, 2, are specified in some parametric way from a family of membership functions, such as triangular or Gaussian. Layer 2 consists of fuzzy neurons with an aggregation operator being some t-norm. We use the product t-norm in this example, in view of the way that product is used in Sugeno-Takagi's inference procedure. The output of Layer 2 is

(O21, O22) = (A1 (x1) B1 (x2), A2 (x1) B2 (x2))

Layer 3 is a normalize. The output of Layer 3 is

$$\begin{aligned}(O_{31}, O_{32}) &= \left(\frac{O_{21}}{O_{21}+O_{22}}, \frac{O_{22}}{O_{21}+O_{22}}\right) \\ &= \left(\frac{A_1(x_1)B_1(x_2)}{A_1(x_1)B_1(x_2)+A_2(x_1)B_2(x_2)}, \frac{A_2(x_1)B_2(x_2)}{A_1(x_1)B_1(x_2)+A_2(x_1)B_2(x_2)}\right)\end{aligned}$$

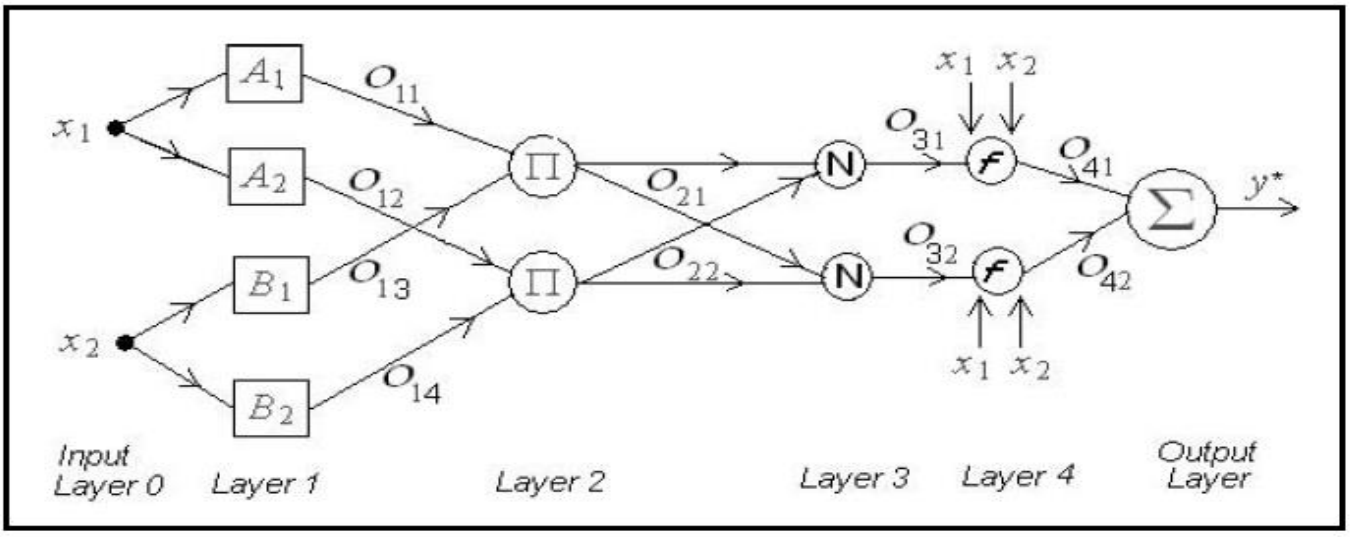

Figure2: First-order Sugeno fuzzy model with two rules

The fuzzy neurons in Layer 4 output the values

$$(O_{41}, O_{42}) = (O_{31} f_1, O_{32} f_2)$$
$$= \left(\frac{(A_1(x_1)B_1(x_2))(z_{11}x_1+z_{12}x_2+z_{13})}{A_1(x_1)B_1(x_2)+A_2(x_1)B_2(x_2)}, \frac{(A_2(x_1)B_2(x_2))(z_{21}x_1+z_{22}x_2+z_{23})}{A_1(x_1)B_1(x_2)+A_2(x_1)B_2(x_2)} \right)$$

Finally, the output layer calculates the control action by summing:

$$y^* = O_{41} + O_{42} = \frac{(A_1(x_1)B_1(x_2))(z_{11}x_1+z_{12}x_2+z_{13})+(A_2(x_1)B_2(x_2))(z_{21}x_1+z_{22}x_2+z_{23})}{A_1(x_1)B_1(x_2)+A_2(x_1)B_2(x_2)}$$

Of course, the above neural network type for representing the inference procedure for a rule base of two rules can be extended in an obvious way to an arbitrary number of rules.

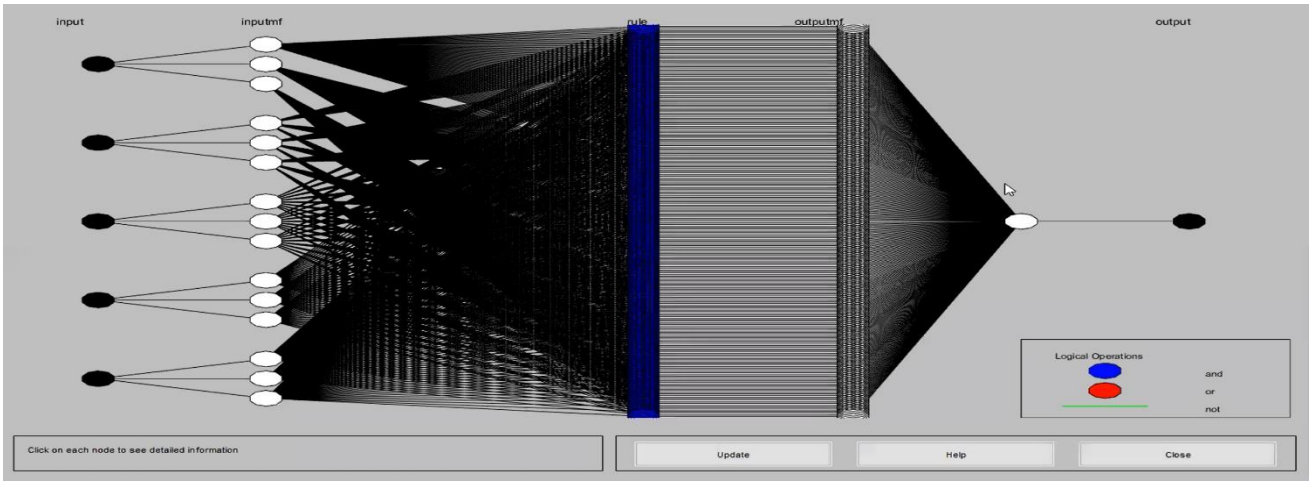

Fig. 3 Fully connected ANFIS 1 structure.

Proposed work:

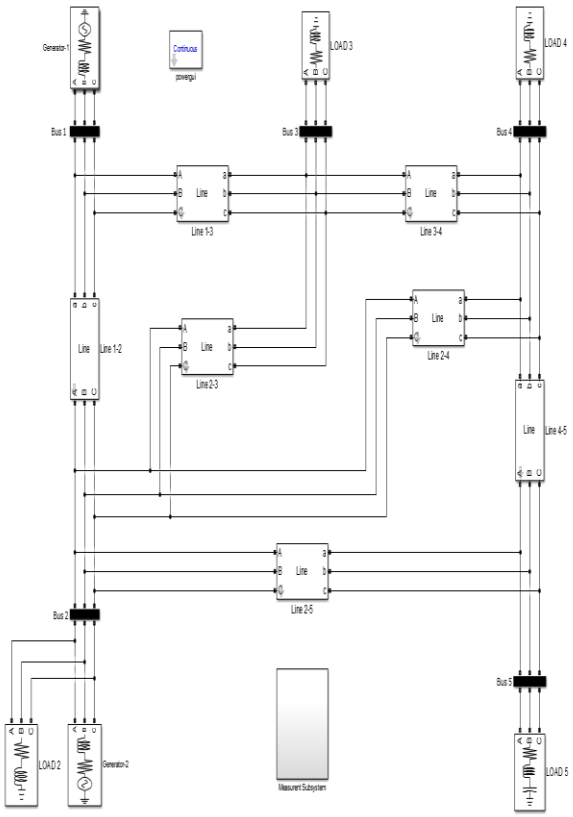

Fig4. IEEE 5 BUS system model

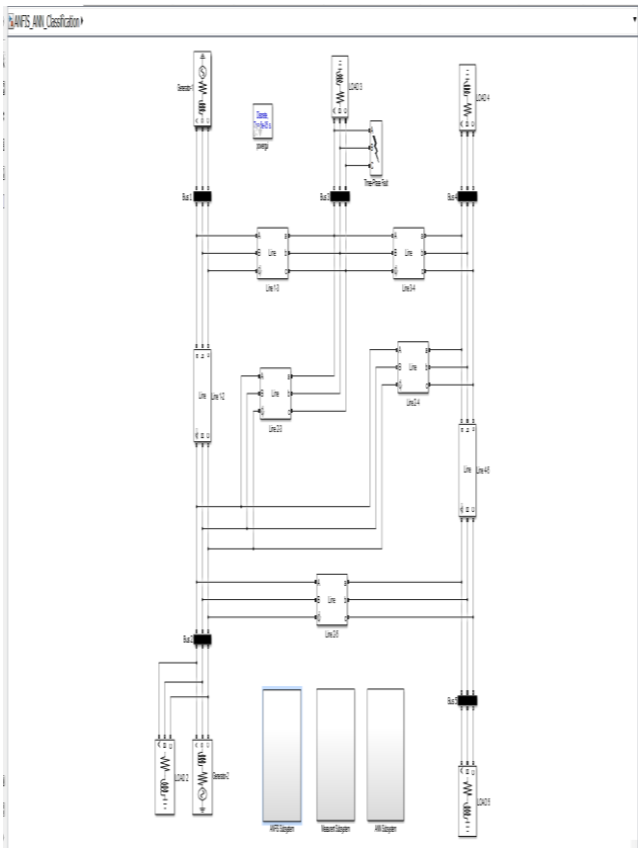

fig5. wavelet-based ANN and ANFIS model

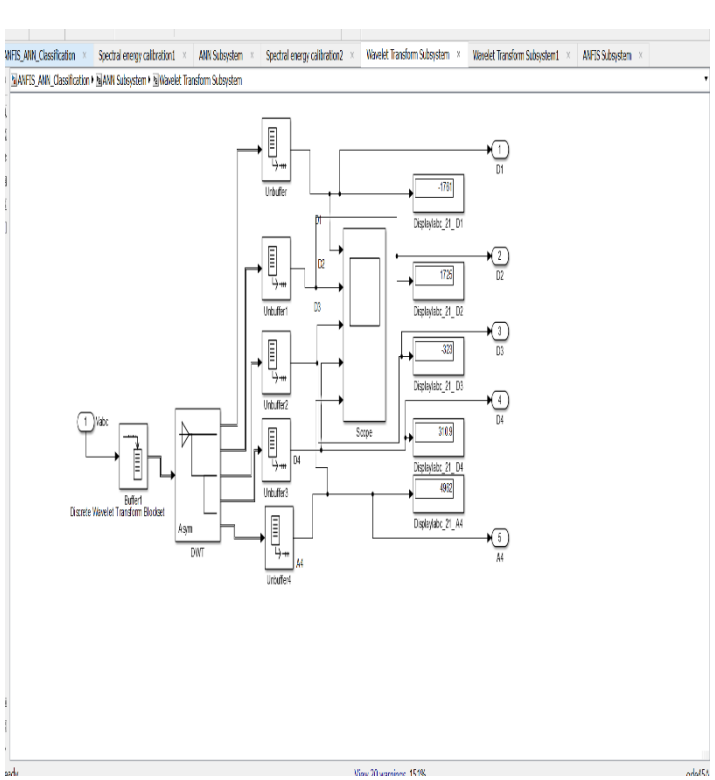

Fig6. wavelet subsystem model

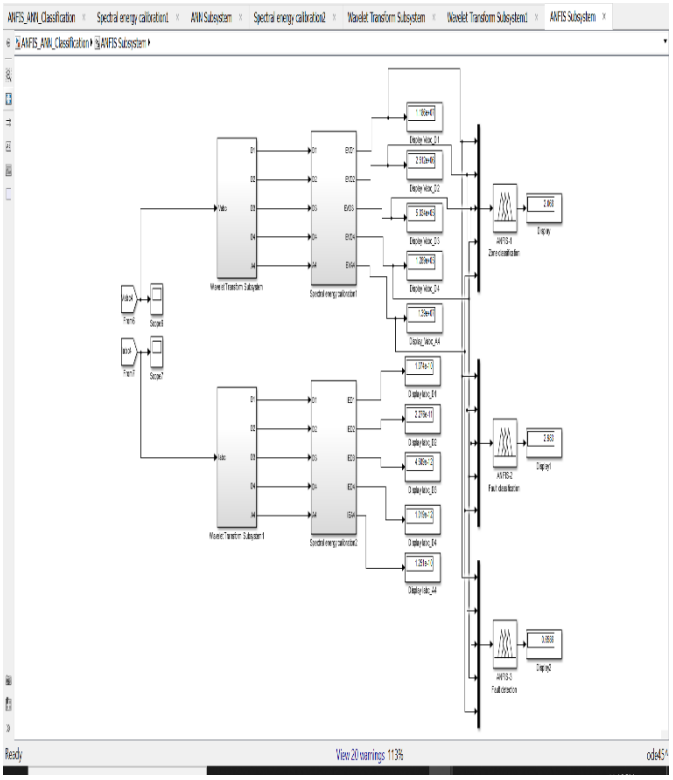

fig.7 ANFIS subsytem model

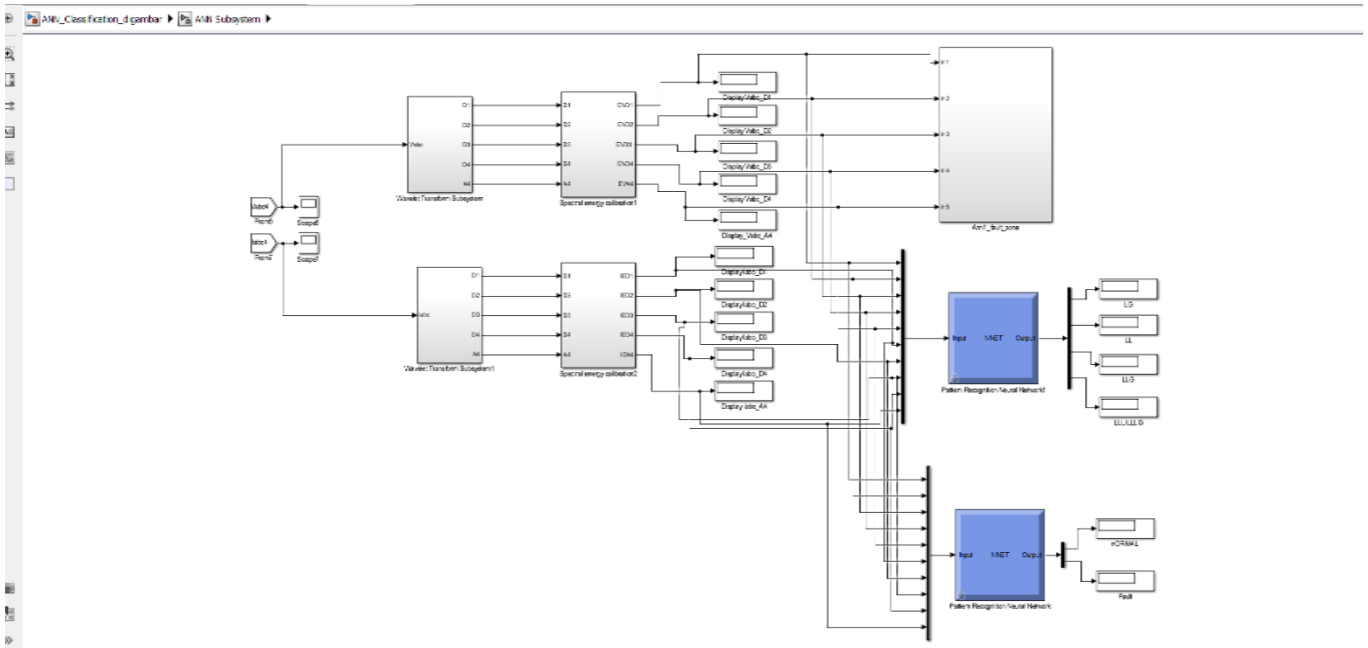

Fig 8. ANN subsystem model

TABLE 1 DATASET FOR ANN AND ANFIS

Work done

Sr No	Location	Fault type	EVD1	EVD2	EVD3	EVD4	EVA4	EID1	EID2	EID3	EID4	DIA4	Bus-1	Bus-2	Bus-3	Bus-4	Bus-5	LG	LL	LLG	LL/LLLG	Normal	Fault
1	Normal	Normal	3.23E+07	6.89E+06	1.34E+06	3.13E+05	3.19E+04	2.32E-10	6.23E-11	1.21E-11	2.83E-12	2.89E-13	0	0	0	0	0	0	0	0	0	1	0
2	Bus-1	AG	2.15E+07	4.56E+06	8.37E+05	2.08E+05	1.43E+07	1.34E-10	4.13E-11	8.11E-12	1.86E-12	1.23E-10	1	0	0	0	0	1	0	0	0	0	1
3	Bus-1	BG	2.14E+07	4.55E+06	8.35E+05	2.14E+05	1.50E+07	1.93E-10	4.11E-11	8.07E-12	1.85E-12	1.35E-10	1	0	0	0	0	1	0	0	0	0	1
4	Bus-1	CG	2.15E+07	4.58E+06	8.39E+05	2.47E+05	1.44E+07	1.95E-10	4.14E-11	8.13E-12	1.87E-12	1.23E-10	1	0	0	0	0	1	0	0	0	0	1
5	Bus-1	AB	1.83E+07	3.87E+06	7.71E+05	1.72E+05	1.39E+04	1.66E-10	3.50E-11	6.37E-12	1.56E-12	1.80E-13	1	0	0	0	0	0	1	0	0	0	1
6	Bus-1	BC	1.84E+07	3.89E+06	7.75E+05	1.74E+05	1.31E+04	1.67E-10	3.51E-11	7.01E-12	1.56E-12	1.76E-13	1	0	0	0	0	0	1	0	0	0	1
7	Bus-1	AC	1.84E+07	3.90E+06	7.77E+05	1.77E+05	1.86E+04	1.67E-10	3.52E-11	7.04E-12	1.57E-12	1.65E-13	1	0	0	0	0	0	1	0	0	0	1
8	Bus-1	ABG	1.22E+07	2.58E+06	5.16E+05	1.45E+05	1.42E+07	1.10E-10	2.34E-11	4.63E-12	1.05E-12	1.28E-10	1	0	0	0	0	0	0	1	0	0	1
9	Bus-1	BCG	1.22E+07	2.60E+06	5.13E+05	1.24E+05	1.44E+07	1.11E-10	2.35E-11	4.65E-12	1.05E-12	1.30E-10	1	0	0	0	0	0	0	1	0	0	1
10	Bus-1	ACG	1.23E+07	2.61E+06	5.16E+05	1.36E+05	1.42E+07	1.11E-10	2.36E-11	4.67E-12	1.06E-12	1.29E-10	1	0	0	0	0	0	0	1	0	0	1
11	Bus-1	ABCG/ABC	4.50E+06	9.68E+05	1.88E+05	4.82E+04	5231	4.09E-11	8.76E-12	1.71E-12	4.02E-13	4.26E-14	1	0	0	0	0	0	0	0	1	0	1
12	Bus-2	AG	1.88E+07	3.98E+06	7.91E+05	1.61E+05	2.55E+07	1.70E-10	3.61E-11	7.15E-12	1.61E-12	2.30E-10	0	1	0	0	0	1	0	0	0	0	1
13	Bus-2	BG	1.87E+07	3.96E+06	7.87E+05	1.83E+05	2.65E+07	1.69E-10	3.58E-11	7.09E-12	1.60E-12	2.40E-10	0	1	0	0	0	1	0	0	0	0	1
14	Bus-2	CG	1.89E+07	4.01E+06	7.99E+05	2.12E+05	2.53E+07	1.71E-10	3.63E-11	7.19E-12	1.63E-12	2.28E-10	0	1	0	0	0	1	0	0	0	0	1
15	Bus-2	AB	1.63E+07	3.39E+06	6.84E+05	1.47E+05	1.84E+04	1.47E-10	3.07E-11	6.28E-12	1.33E-12	1.61E-13	0	1	0	0	0	0	1	0	0	0	1
16	Bus-2	BC	1.64E+07	3.42E+06	7.01E+05	1.50E+05	1.88E+04	1.48E-10	3.09E-11	6.33E-12	1.34E-12	1.61E-13	0	1	0	0	0	0	1	0	0	0	1
17	Bus-2	AC	1.65E+07	3.44E+06	7.05E+05	1.54E+05	1.72E+04	1.49E-10	3.11E-11	6.37E-12	1.35E-12	1.53E-13	0	1	0	0	0	0	1	0	0	0	1
18	Bus-2	ABG	8.24E+06	1.72E+06	3.69E+05	9.69E+04	2.49E+07	7.48E-11	1.56E-11	3.19E-12	6.82E-13	2.24E-10	0	1	0	0	0	0	0	1	0	0	1
19	Bus-2	BCG	8.31E+06	1.74E+06	3.55E+05	8.40E+04	2.51E+07	7.52E-11	1.57E-11	3.21E-12	6.30E-13	2.62E-10	0	1	0	0	0	0	0	1	0	0	1
20	Bus-2	ACG	8.34E+06	1.75E+06	3.59E+05	9.35E+04	2.52E+07	7.57E-11	1.59E-11	3.23E-12	6.39E-13	2.28E-10	0	1	0	0	0	0	0	1	0	0	1
21	Bus-2	ABCG/ABC	4.64E+05	1.03E+05	2.26E+04	1.01E+04	1356	4.44E-12	9.80E-13	1.93E-13	4.37E-14	7.47E-15	0	1	0	0	0	0	0	0	1	0	1
22	Bus-3	AG	2.13E+07	4.53E+06	8.91E+05	2.06E+05	1.41E+07	1.93E-10	4.10E-11	8.05E-12	1.85E-12	1.27E-10	0	0	1	0	0	1	0	0	0	0	1
23	Bus-3	BG	2.12E+07	4.51E+06	8.88E+05	2.08E+05	1.49E+07	1.92E-10	4.08E-11	8.00E-12	1.84E-12	1.34E-10	0	0	1	0	0	1	0	0	0	0	1
24	Bus-3	CG	2.14E+07	4.55E+06	8.92E+05	2.27E+05	1.42E+07	1.93E-10	4.11E-11	8.07E-12	1.86E-12	1.27E-10	0	0	1	0	0	1	0	0	0	0	1
25	Bus-3	AB	1.81E+07	3.81E+06	7.53E+05	1.63E+05	1.96E+04	1.63E-10	3.44E-11	6.87E-12	1.53E-12	1.77E-13	0	0	1	0	0	0	1	0	0	0	1
26	Bus-3	BC	1.82E+07	3.83E+06	7.64E+05	1.71E+05	1.94E+04	1.64E-10	3.46E-11	6.91E-12	1.54E-12	1.74E-13	0	0	1	0	0	0	1	0	0	0	1
27	Bus-3	AC	1.82E+07	3.84E+06	7.65E+05	1.74E+05	1.81E+04	1.65E-10	3.47E-11	6.94E-12	1.55E-12	1.63E-13	0	0	1	0	0	0	1	0	0	0	1
28	Bus-3	ABG	1.19E+07	2.51E+06	5.03E+05	1.29E+05	1.39E+07	1.07E-10	2.28E-11	4.51E-12	1.02E-12	1.25E-10	0	0	1	0	0	0	0	1	0	0	1
29	Bus-3	BCG	1.19E+07	2.53E+06	5.00E+05	1.18E+07	1.41E+07	1.08E-10	2.29E-11	4.53E-12	1.03E-12	1.21E-10	0	0	1	0	0	0	0	1	0	0	1
30	Bus-3	ACG	1.20E+07	2.54E+06	5.02E+05	1.24E+05	1.40E+07	1.08E-10	2.30E-11	4.55E-12	1.04E-12	1.26E-10	0	0	1	0	0	0	0	1	0	0	1
31	Bus-3	ABCG/ABC	3.95E+06	8.51E+05	1.66E+05	4.22E+04	4.57E-03	3.60E-11	7.72E-12	1.51E-12	3.56E-13	3.80E-14	0	0	1	0	0	0	0	0	1	0	1
32	Bus-4	AG	1.81E+07	3.83E+06	7.63E+05	1.70E+05	3.04E+07	1.93E-03	4.06E-10	8.12E-11	1.79E-11	4.26E-03	0	0	0	1	0	1	0	0	0	0	1
33	Bus-4	BG	1.80E+07	3.80E+06	7.59E+05	1.63E+05	3.16E+07	1.95E-03	4.10E-10	8.23E-11	1.81E-11	4.34E-03	0	0	0	1	0	1	0	0	0	0	1
34	Bus-4	CG	1.82E+07	3.84E+06	7.67E+05	1.82E+05	3.02E+07	1.90E-03	4.00E-10	8.01E-11	1.77E-11	4.24E-03	0	0	0	1	0	1	0	0	0	0	1
35	Bus-4	AB	1.62E+07	3.35E+06	6.75E+05	1.44E+05	1.85E+04	3.59E-03	7.52E-10	1.52E-10	3.29E-11	3.70E-12	0	0	0	1	0	0	1	0	0	0	1
36	Bus-4	BC	1.63E+07	3.38E+06	6.39E+05	1.45E+05	1.32E+04	3.54E-03	7.41E-10	1.50E-10	3.25E-11	3.53E-12	0	0	0	1	0	0	1	0	0	0	1
37	Bus-4	AC	1.63E+07	3.38E+06	7.00E+05	1.46E+05	1.75E+04	3.50E-03	7.32E-10	1.48E-10	3.20E-11	3.95E-12	0	0	0	1	0	0	1	0	0	0	1
38	Bus-4	ABG	7.50E+06	1.56E+06	3.26E+05	6.35E+04	2.36E+07	4.15E-03	8.73E-10	1.74E-10	3.34E-11	4.05E-03	0	0	0	1	0	0	0	1	0	0	1
39	Bus-4	BCG	7.55E+06	1.57E+06	3.24E+05	7.04E+04	2.39E+07	4.11E-03	8.70E-10	1.72E-10	3.90E-11	4.10E-03	0	0	0	1	0	0	0	1	0	0	1
40	Bus-4	ACG	7.56E+06	1.58E+06	3.25E+05	7.27E+04	3.02E+07	4.06E-03	8.53E-10	1.69E-10	3.84E-11	4.33E-03	0	0	0	1	0	0	0	1	0	0	1
41	Bus-4	ABCG/ABC	1.81E+05	4.66E+04	9331	2725	1463	6.78E-03	1.45E-03	2.81E-10	6.56E-11	6.63E-12	0	0	0	1	0	0	0	0	1	0	1
42	Bus-5	AG	2.35E+07	5.02E+06	9.82E+05	2.26E+05	1.61E+06	2.13E-10	4.54E-11	8.86E-12	2.06E-12	6.86E-11	0	0	0	0	1	1	0	0	0	0	1
43	Bus-5	BG	2.35E+07	5.00E+06	9.78E+05	2.28E+05	8.13E+06	2.12E-10	4.52E-11	8.83E-12	2.06E-12	7.34E-11	0	0	0	0	1	1	0	0	0	0	1
44	Bus-5	CG	2.36E+07	5.03E+06	9.84E+05	2.38E+05	7.65E+06	2.13E-10	4.55E-11	8.90E-12	2.05E-12	6.88E-11	0	0	0	0	1	1	0	0	0	0	1
45	Bus-5	AB	2.03E+07	4.31E+06	8.43E+05	1.94E+05	2.13E+04	1.84E-10	3.90E-11	7.68E-12	1.76E-12	1.92E-13	0	0	0	0	1	0	1	0	0	0	1
46	Bus-5	BC	2.04E+07	4.33E+06	8.54E+05	1.93E+05	2.10E+04	1.84E-10	3.92E-11	7.71E-12	1.76E-12	1.90E-13	0	0	0	0	1	0	1	0	0	0	1
47	Bus-5	AC	2.04E+07	4.34E+06	8.57E+05	1.92E+05	1.98E+04	1.85E-10	3.93E-11	7.73E-12	1.77E-12	1.80E-13	0	0	0	0	1	0	1	0	0	0	1
48	Bus-5	ABG	1.56E+07	3.32E+06	6.54E+05	1.56E+05	7.58E+06	1.41E-10	3.00E-11	5.88E-12	1.37E-12	6.32E-11	0	0	0	0	1	0	0	1	0	0	1
49	Bus-5	BCG	1.56E+07	3.33E+06	6.55E+05	1.52E+05	7.69E+06	1.42E-10	3.01E-11	5.91E-12	1.36E-12	6.33E-11	0	0	0	0	1	0	0	1	0	0	1
50	Bus-5	ACG	1.57E+07	3.34E+06	6.57E+05	1.52E+05	7.49E+05	1.42E-10	3.02E-11	5.93E-12	1.36E-12	6.77E-11	0	0	0	0	1	0	0	1	0	0	1
51	Bus-5	ABCG/ABC	8.47E+06	1.81E+06	3.55E+05	8.10E+04	8742	7.69E-11	1.65E-11	3.20E-12	7.51E-13	7.78E-14	0	0	0	0	1	0	0	0	1	0	1

Data set for ANN AND ANFIS

In this project IEEE5 bus system is simulated in matlab 2016, for anlysis of fault wavelet-based ANN and ANFIS is applied on model. Fig.4 shows IEEE5 bus system. Fig.5 shows complete model with wavelet subsystem model, ANN0 model and ANFIS model. In fig. 6 wavelet subsystem is connected continues waveform of Vabc and Iabc is converted into discrete waveform and after that DWT (discrete wavelet transform) is applied. But after DWT waveform is converted into continues signal to calculate the result from DWT.

For giving a steady constant result to ANN and ANFIS, DWT is converted energy signal. Fig.7 shows ANFIS model in that 3 ANFIS is applied. On which 1st ANFIS is for identify location of fault, 2nd is for identify the fault on system and 3rd ANFIS is for diagnosed fault or normal condition. In same way ANN is connected which is show in fig.8

RESULT:

NOEMAL CONDITON:

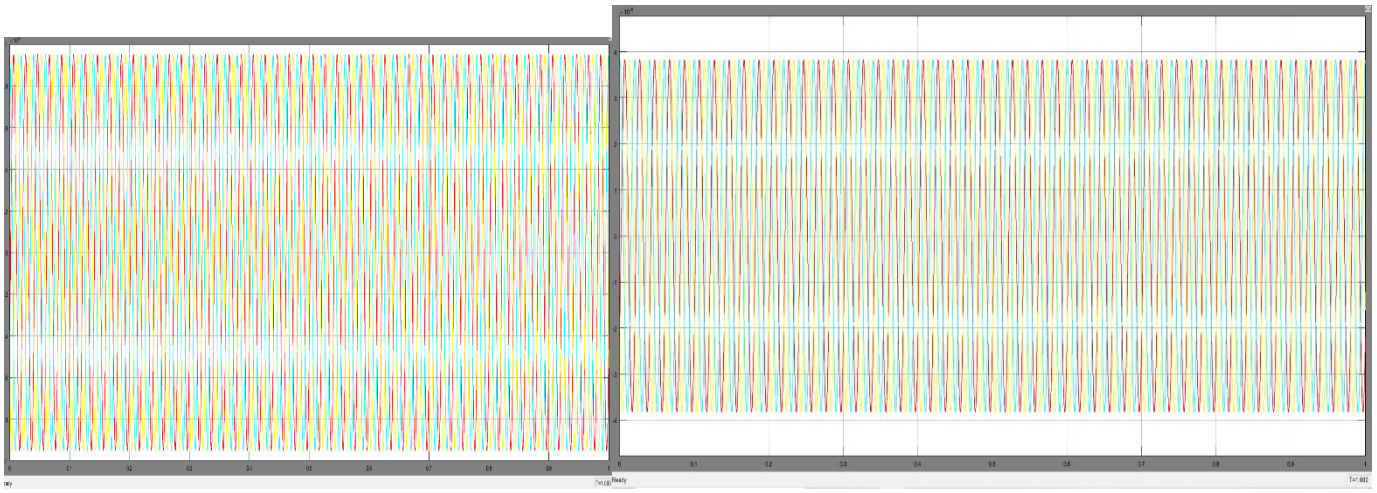

FIG.9 VOLTAGE Vabc AND CURENT Iabc waeform

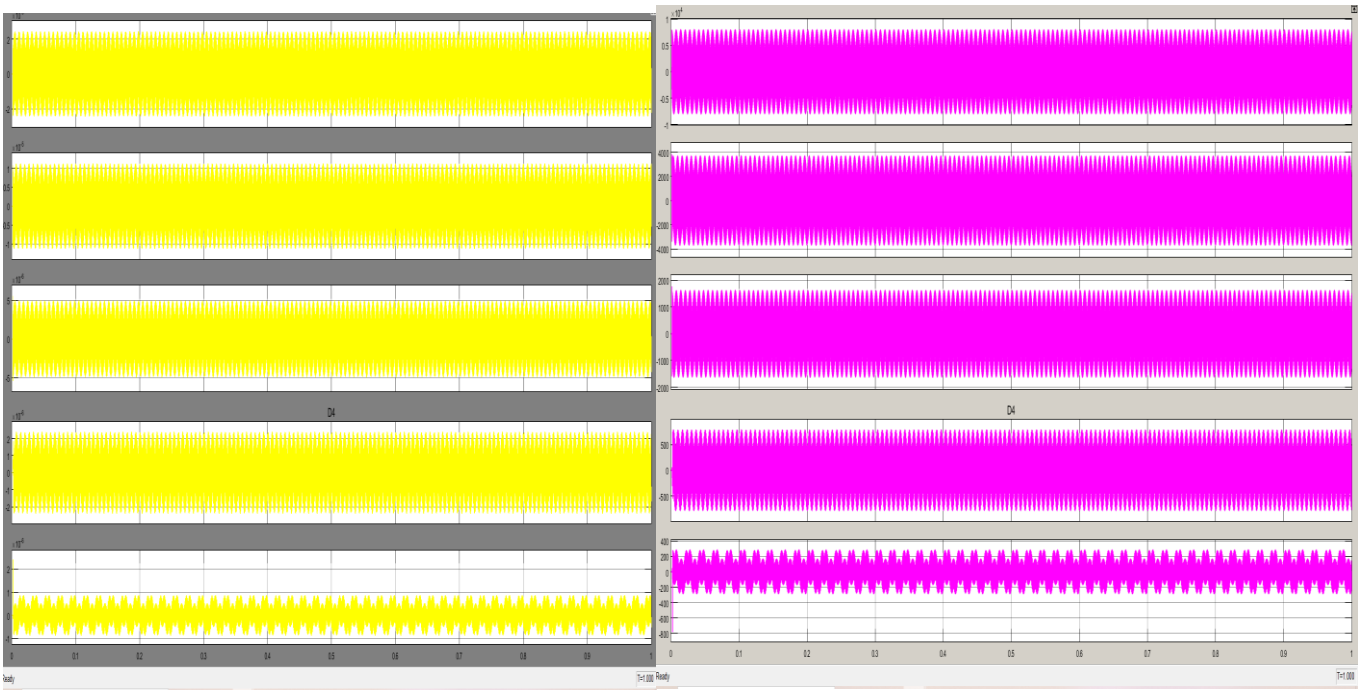

Fig.10 wavelet DWT of voltage and current

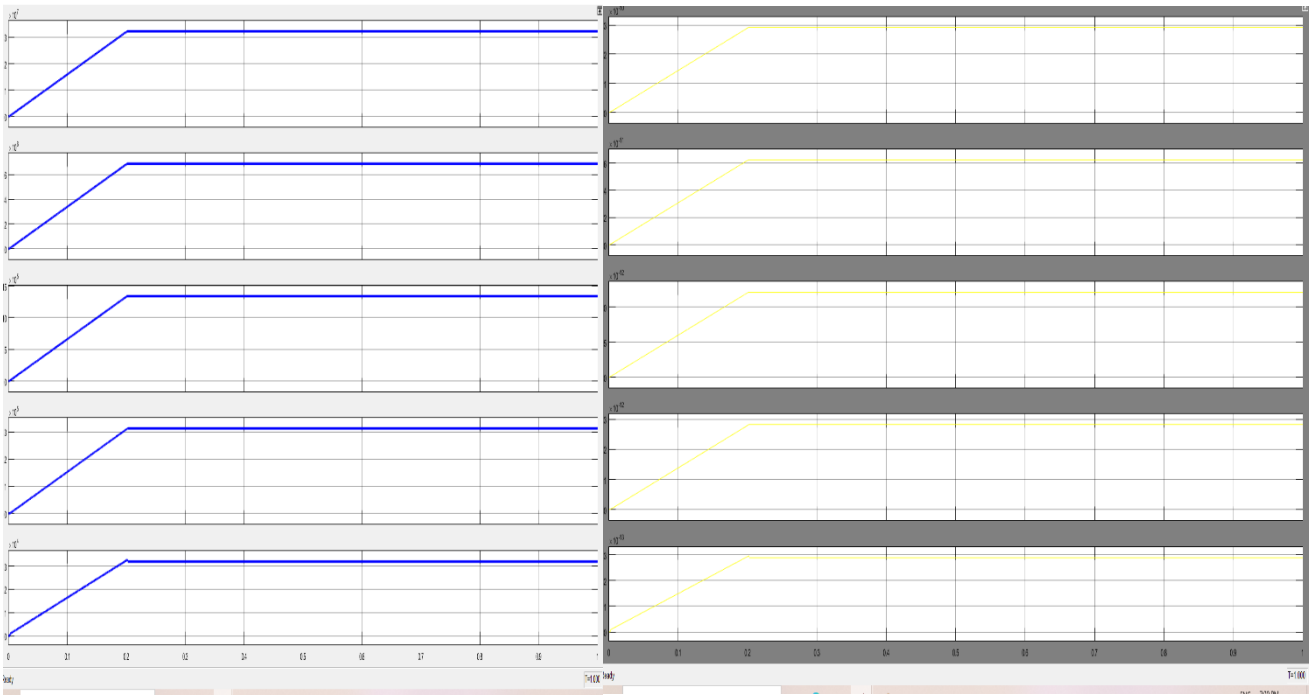

Fig.11 energy waveform of current and voltage

Fault condition

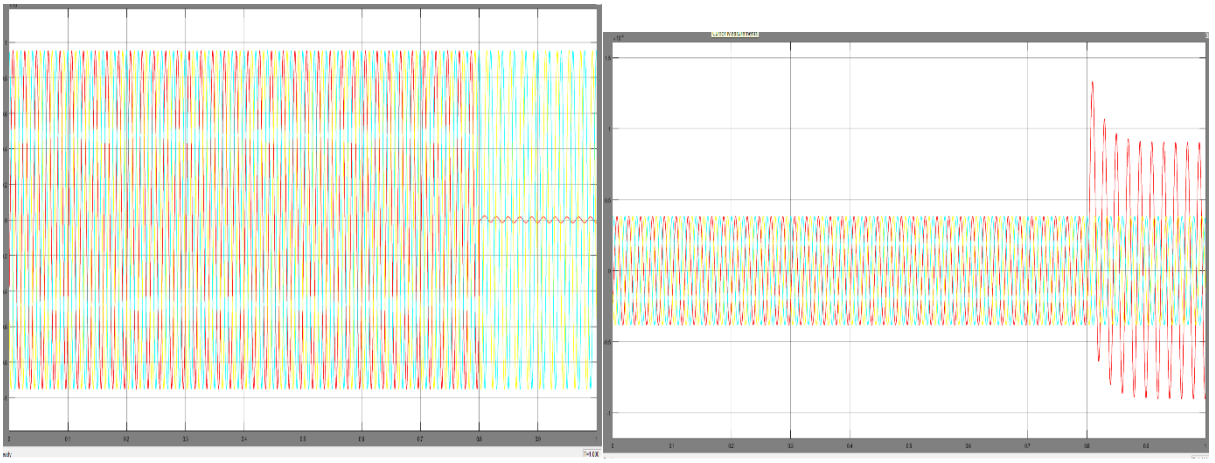

Fig.12 Vabc and Iabc at zone1 LG fault

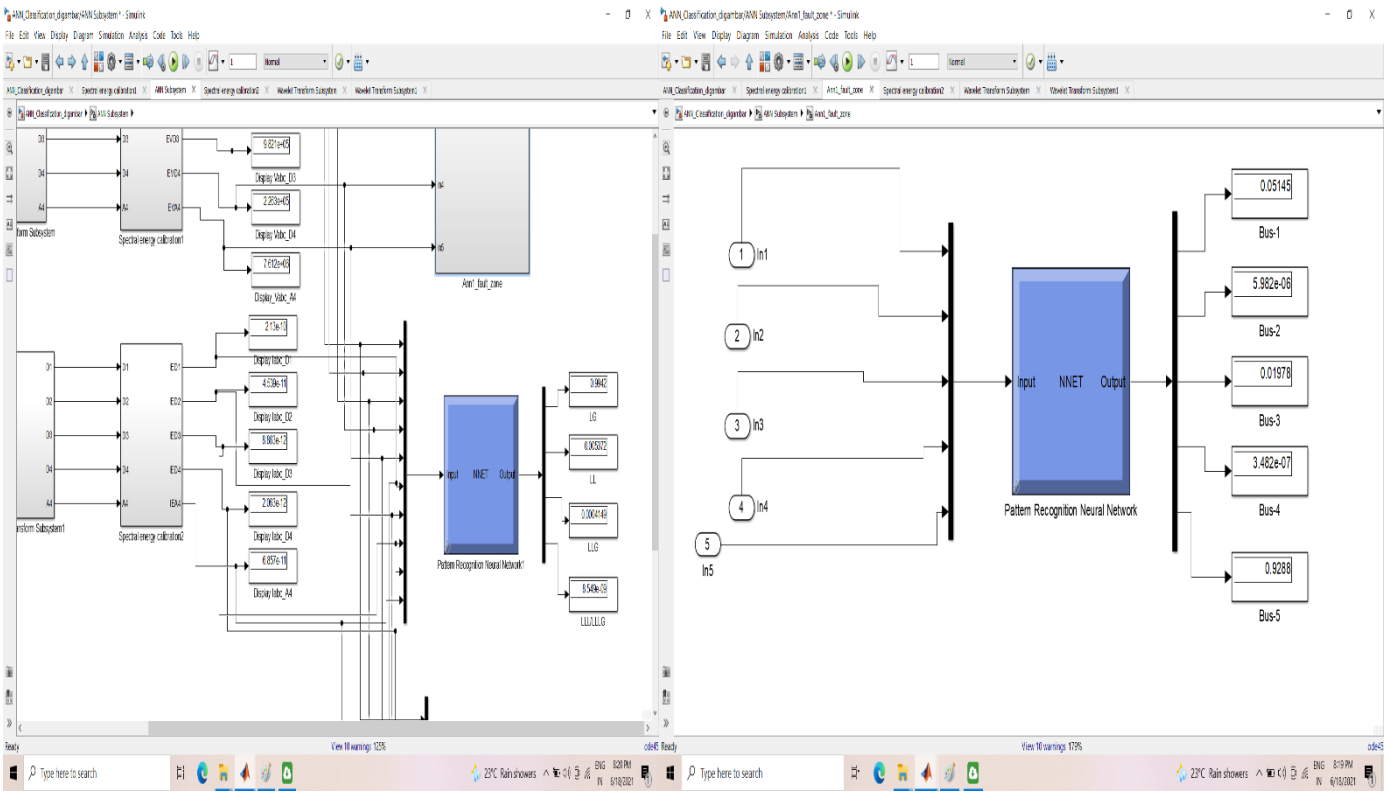

FIG.13 ANN SHOWS LG FAULT AND FAULT AT BUS 5

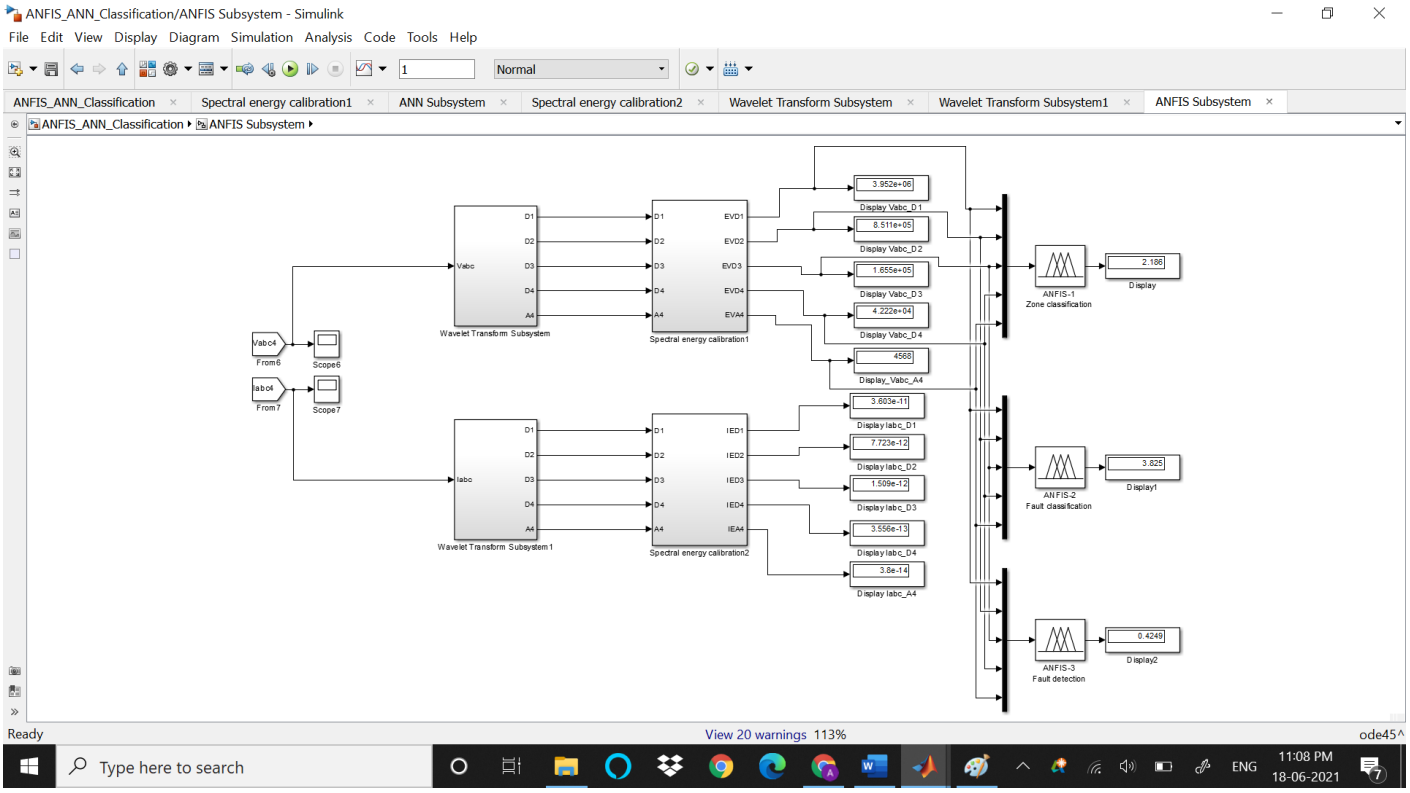

FIG.14 ANFIS SHOW LLG fault and on bus 5.

fig 9 to fig. 14 shows result waveform of fault condition and normal condition. From the result we get 51 different cases viz. LG FAULT (3 TYPES), LL FAULT (3 TYPES), LLG FAULT (3 TYPE), LLLLG/LLLL FAULT AND NORMAL CONDITION. All this fault is taken on 5 buses so it will be total 51 cases. All these 51 cases are experimented on IEEE 5 BUS system with discrete based ANN and ANFIS.

CONCLUSION:

The proposed method is based on wavelet transform and a new classifier named as Artificial Neural Network (ANN) and wavelet transform. The proposed method is implemented on a 5 bus IEEE bus grid in MATLAB/SIMULINK software. The results show the high accuracy of fault detection of the proposed method. In this paper, 5 bus is considered, in which different fault is taken and this fault is localized, identified by the wavelt analysis, ANN technique and ANFIS technic. This method implemented for classify or detection of fault in IEEE 14 bus system. In this paper we were classify the fault using ANN and ANFIS classifier. It is observed that ANN classify the event of islanding up to 90% while ANFIS classify the event of FAULT up to 74.3%. Hence it is clear that ANN provide best classification results for detection of FAULT number event.

References:

[1] S. Parhizi, H. Lotfi, A. Khodaei, and S. Bahramirad, "State-of-the-art in research on microgrids: A review," IEEE Access, vol. 3, pp. 890–925, 2015.

[2] Y. Y. Hong, Y. H. Wei, Y. R. Chang, Y. D. Lee, and P. Liu, "Fault detection and location by static switches in microgrids using wavelet transform and adaptive network-based fuzzy inference system," Energies, vol. 7, no. 4, pp. 2658–2675, 2014.

[3] S. Kar and S. R. Samantaray, "High impedance fault detection in microgrid using maximal overlapping discrete wavelet transform and decision tree," in Proc. 6th Int. Conf. Electr. Power Energy Syst., Paris, France, 2016, pp. 258–263.

[4] B. K. Panigrahi, P. K. Ray, P. K. Rout, and S. K. Sahu, "Detection and location of fault in a micro grid using wavelet transform," Proc. Int. Conf. Circuit, Power Comput. Technol., Kollam, India, 2017.

[5] T. Considine, W. Cox, and E. G. Cazalet, "Understanding microgrids as the essential architecture of smart energy," in Proc. Grid-Interop Forum, Irving, TX, USA, 2012.

[6] D. P. Mishra, S. R. Samantaray, and G. Joos, "A combined wavelet and data-mining based intelligent protection scheme for microgrid," IEEE Trans. Smart Grid, vol. 7, no. 5, pp. 2295–2304, Sep. 2016.

[7] M. Mao, Y. Tao, L. Chang, Y. Zhao, and P. Jin, "An intelligent static switch based on embedded system and its control method for a microgrid," in Proc. IEEE PES Innov. Smart Grid Technol., Tianjin, China, 2012.

[8] M. Mishra and P. K. Rout, "Detection and classification of micro-grid faults based on HHT and machine learning techniques," IET Gener. Transmits. Diatribe., vol. 12, no. 2, pp. 388–397, 2018.

[9] B. Kroposki et al., "Development of a high-speed static switch for dis- tributed energy and microgrid applications," in Proc. Power Convers. Conf., Nagoya, Japan, Apr. 2–5, 2007, pp. 1418–1423.

[10] Y. Y. Hong, J. L. Gu, and F. Y. Hsu, "Design and realization of controller for static switch in microgrid using wavelet-based TSK reasoning," IEEE Trans. Ind. Inform., vol. 14, no. 11, pp. 4864–4872, Nov. 2018.

[11] J. J.Q. Yu, Y. Hou, A.Y.S. Lam, and V.O. K. Li, "Intelligent fault detection scheme for microgrids with wavelet-based deep neural networks," IEEE Trans. Smart Grid, vol. 10, no. 2, pp. 1694–1703, Mar. 2019.

[12] M. A. Jarrahi, H. Samet, and T. Ghanbari, "Fast current-only based fault detection method in transmission line," IEEE Syst. J., vol. 13, no. 2, pp. 1725–1736, Apr. 2018.

[13] Z. Y. Jiang, Z. W. Li, N. Q. Wu, and M. C. Zhou, "A Petri net ap- proach to fault diagnosis and restoration for power transmission systems to avoid the output interruption of substations," IEEE Syst. J., vol. 12, no. 3, pp. 2566–2576, Sep. 2018.

[14] R. Dubey, S. R. Samantaray, B. K. Panigrahi, and V. G. Venkoparao, "Koopman analysis based wide-area back-up protection and faulted line identification for series-compensated power network," IEEE Syst. J., vol. 12, no. 3, pp. 2634–2644, Sep. 2018.

[15] N. Geddada, Y. M. Yeap, and A. Ukil, "Experimental validation of fault identification in VSC-based DC grid system," IEEE Trans. Ind. Electron.," vol. 65, no. 6, pp. 4799–4809, Jun. 2018.